Preprints.org

Article

Phytoplankton Bloom Localized by Sentinel-2 Images and Hydrodynamic Modelling – Sulejów Reservoir, Pilica River, Poland

Peshang Hama Karim , Monika Kalinowska , Aleksandra Zieminska-Stolarska , Artur Magnuszewski [*]

Article

Phytoplankton Bloom Localized by Sentinel-2 Images and Hydrodynamic Modelling - Sulejów Reservoir, Pilica River, Poland

Peshang Hama Karim [1], Monika Kalinowska [2], Aleksandra Zieminska-Stolarska [3] and Artur Magnuszewski [4,*]

[1] Doctoral School of Exact and Natural Sciences, Discipline of Earth and related Environmental Sciences, University of Warsaw, ul. S. Banacha 2c, 02-097 Warszawa; peshang.hamakarim@student.uw.edu.pl

[2] Institute of Geophysics, Polish Academy of Sciences, Księcia Janusza 64, 01-452 Warszawa; mkalinow@igf.edu.pl

[3] Faculty of Process and Environmental Engineering, Technical University of Lodz, Wólczańska 213, 93-005 Łódź; aleksandra.zieminska-stolarska@p.lodz.pl

[4] Faculty of Geography and Regional Studies, University of Warsaw, Krakowskie Przedmieście 30, 00-927 Warszawa; asmagnus@uw.edu.pl

* Correspondence: asmagnus@uw.edu.pl

Abstract: Reservoirs created by damming rivers significantly modify the environment and problems may arise: the storage of nutrients and organic matter in reservoirs often leads to decreased water quality due to eutrophication. Reservoirs built on lowland rivers are exposed to significant nutrient loads, often leading to eutrophication. In this article, the Sulejów Reservoir, in Central Poland, was the subject of the research, which focused on the use of Sentinel-2 remote sensing data to detect phytoplankton blooms, and on understanding the pattern of wind-driven surface currents using the CCHE2D model (a depth-averaged hydrodynamic model). The calculation of the total phosphorus load has shown that the reservoir mainly acts as nutrient storage. Still, during the low flow and intensive phytoplankton bloom, it can be a source of nutrients. The distribution of phytoplankton bloom on the Sulejów Reservoir was documented using eight Sentinel-2 satellite images from the vegetation season of 2020 and the Normalized Difference Chlorophyll Index (NDCl). Coupling remote sensing data and numerical modelling helps to interpret the hydrodynamic model results and understand nutrients and sediment dynamics within the reservoir. Hydrodynamic modelling combined with remote sensing data can be a valuable tool for selecting appropriate locations for water quality measurements at monitoring stations.

Keywords: eutrophication; phytoplankton blooms; Sentinel-2; hydrodynamic modelling; Pilica River; Sulejow Reservoir; NDCl; CCHE2D

1. Introduction

Rivers transport not only water but also solutes and sediments from their catchments. In recent water management and environmental protection measures, special consideration has been given to the load of nutrients transported by municipal sewage and generated by agriculture as non-point sources. High nutrient concentrations are responsible for eutrophication processes in natural lakes, artificial reservoirs, and coastal sea waters. Phytoplankton, having access to nutrients transported by the river flow, and finding favourable conditions of stagnant and warm water in reservoirs or lakes, may produce a high concentration, counted in millions of cells per 1 cm3 of water. Phytoplankton bloom results from eutrophication, defined as excessive productivity in aquatic ecosystems [1]. The concept and definition of eutrophication have developed from studies of limnology and ecology. One of the first papers on eutrophication related to massive algae blooms on Lake Haruna (Japan) at the end of 1992 [2] after [3]. The driving factor of lake eutrophication, as manifested by phytoplankton bloom, is phosphorus flux [4]. The transport of phosphorus in river systems is related to sediment movement, starting from slope erosion, through the suspended sediments transported in moving water, and, finally, to bottom sediments. Two forms of phosphorus are measured at water quality

monitoring stations – dissolved phosphate ions and total phosphorus. Total phosphorus (TP) measures all phosphorus found in a sample, both dissolved and particulate (organic). TP is commonly used when sampling water quality and determining the ecological status of water.

Phytoplankton blooms are composed of a mixture of cyanobacteria and algae. The occurrence of cyanobacterial (blue-green algal) blooms in artificial reservoirs is of global concern. Sulejów Reservoir experiences blue-green algal blooms every year, all having the ability to produce cyanotoxins [5]. Cyanotoxins, as secondary metabolites, affect aquatic organisms at all taxonomic levels, including different groups of algae, macrophytes, zooplankton, and fish [6].

Artificial reservoirs on lowland rivers are exposed to eutrophication processes due to the high flux of nutrients from a large catchment, the long retention time, and the dominating sedimentation in a lacustrine part of the reservoir. Easily available nutrients are used in primary biological production, resulting in phytoplankton bloom, which is dominated in summer by cyanobacteria [7].

The phytoplankton blooms can be observed from satellite platforms equipped with multispectral scanners. The major techniques are based on optical sensing through the detection of coloured phytoplankton pigments (MODIS, MERIS, Landsat, Sentinel-2), together with thermal sensing of water temperature (AVHRR) [8].

The use of remote sensing brings several advantages: (1) it provides a synoptic view of the study site, which allows the user to retrieve information on the entire aquatic system surface; (2) it can acquire data from remote, inaccessible locations; and (3) it can record data over time, providing a historical dataset for more comprehensive monitoring [9,10].

The modelling results show that multispectral sensors, such as ALI, Landsat, and MODIS, are not capable of distinguishing waters dominated by cyanobacteria from waters dominated by other algae species, as their spectral band configuration does not allow absorption features caused by phycocyanin (present primarily in cyanobacteria), or any other spectral features that are characteristic of cyanobacteria only, to be detected. MERIS bands B6 and B7 allow for the detection of phycocyanin absorption features near 630 nm, and a small peak in reflectance spectra near 650 nm, which is characteristic of cyanobacteria only. Thus, MERIS can be used to detect cyanobacteria if they are present in relatively high quantities. Unfortunately, it is not possible to use MERIS for early warning of potentially harmful emerging blooms as the minimum biomass needed to cause features in reflectance spectra typical of cyanobacteria is higher than the biomass already considered as bloom in the Baltic Sea [11].

To detect phytoplankton bloom on Sentinel-2 multispectral satellite images, the Normalized Difference Chlorophyll index (NDCl) was applied to images over Chesapeake Bay, Delaware Bay, Mobile Bay, and the Mississippi River delta region in the northern Gulf of Mexico. The newly developed algorithm successfully predicted Chl-a concentration, with approximately 12% overall bias for all the above study regions. Findings from this research imply that NDCl can be successfully used on MERIS images to monitor Chl-a in inland, coastal, and estuarine waters quantitatively. In the case of remote coastal waters with no ground truth data, NDCl can be used to detect algal bloom and qualitatively infer Chl-a concentration ranges that are very similar to NDVI application in terrestrial vegetation studies [12].

Blooms form when there is a high concentration of algae within a particular lake area, accompanied by some form of the physical mechanism that concentrates cells further [13]. Lakes with high retention times offer favourable conditions for blue-green algae bloom because cyanobacteria have slow growth rates relative to other algal groups [14]. Also, water column stability is important because cyanobacteria can regulate their buoyancy and depth of submergence, maintaining optimal position in the water column for light harvesting. Another parameter that increases cyanobacteria concentration is a high water temperature of 15–50°C. However, cyanobacteria are very sensitive to the rapid cooling of the water. Lowering the temperature by 5°C in a few days may destroy the bloom [7].

Additionally, due to low velocity in the lacustrine parts of a reservoir, the pattern of blue-green algae is controlled by the water currents and wind drift. These processes create complicated velocity fields, which can be obtained by applying two-dimensional hydrodynamic modelling. The results of

hydrodynamic modelling can explain many important hydrological determinants in lakes, such as hydraulic residence time, surface circulation pattern, and velocity distribution [15–18].

Various hydrodynamic models of different dimensions may be considered for studying flow dynamics and sedimentation processes. One-dimensional (1D) models, such as HEC-RAS, are commonly utilized to calculate key hydraulic parameters in cross-sections, such as water level, area, velocity, and shear stress. For instance, [19] employed HEC-RAS to delineate the riverine, transitional, and lacustrine zones in the Sulejów reservoir, aiding in the understanding of the longitudinal gradients of water quality parameters from the backwater area to the dam.

Moreover, the use of two-dimensional (2D) models, exemplified by the CCHE2D model, has been prominent in studying flow and sedimentation processes in large reservoirs in Poland, as demonstrated by [20,21]. Unlike 1D models, which primarily calculate parameters in cross-sections, CCHE2D allows for a more comprehensive analysis by considering spatial variations in water flow.

Furthermore, three-dimensional (3D) hydrodynamic models, such as the one developed by [22], offer even more detailed insights into velocity patterns, showing the complex pattern of wind-driven water circulation in the lacustrine zone.

In this paper, we focus on the application of a 2D hydrodynamic model, namely CCHE2D, to analyse flow dynamics in the studied reservoir. This choice aligns with the objectives of our research. In addition to its foundational capabilities in simulating water flow and sediment transport, CCHE2D is distinguished by its ability to incorporate the influence of wind in its computations. This feature allows the model to account for the impact of wind on water surfaces, contributing to a more comprehensive representation of natural hydrodynamic processes.

2. Materials and Methods

2.1. Study area

The Pilica River is the biggest tributary on the left bank of the Vistula River in Poland. It stretches for 342 kilometres and has a catchment area of 9258 km2 (Figure 1). The reservoir was built between 1969 and 1973 to provide a drinking water supply for the fast-expanding metropolis of Łódź, situated about 50 kilometres northwest of the reservoir.

The Sulejów Reservoir has an earth dam, located in Smardzewice village, measuring 15.4 metres in height and spanning 1210 metres in length. The reservoir is 15.5 kilometres long, has a maximum width of 2.1 kilometres, and covers a surface area of 22 square kilometres. The reservoir's capacity is used for flood management, and it has an 8.5 m water head that powers a hydropower plant equipped with two 1.7 MW Kaplan turbines. Agricultural activities cover 60% of the Pilica River watershed area, with forests occupying 31%. The Pilica River catchment, especially the Sulejów Reservoir's differential catchment, experiences substantial human-induced pressure, marked by the highest population density and the largest volume of water discharged from municipal water treatment facilities in the entire Pilica River catchment [23].

The two main rivers supplying Sulejów Reservoir are Pilica and its left tributary Luciąża. The long-term average discharge of Pilica at Sulejów gauge is 22.8 m³s⁻¹, and of Luciąża at Kłudzice is 3.03 m³s⁻¹. The water turnover in the Sulejów Reservoir is long, with an average discharge of more than 30 days. This feature enhances the sedimentation processes through stable hydrodynamic conditions in the reservoir.

Although the reservoir has a large volume, sedimentation is not very intense. [24] determined that 46,000 cubic meters of water were lost annually over 50 years of reservoir use.
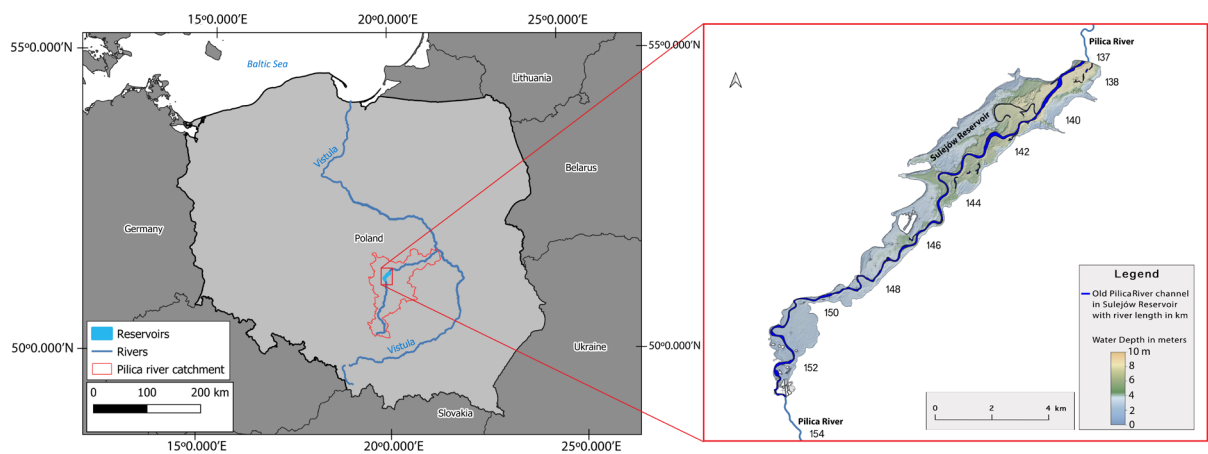
Figure 1. Location of the Sulejów Reservoir on the Pilica River.

The occurrence of blue-green algae has been observed every year since the reservoir began operating and was one of the reasons for closing the surface water intake for the Łódź city waterworks. Sulejów Reservoir is supplied at the inlet (backwater area) by the Pilica River and Luciąża River; both rivers are controlled by hydrological gauges (Sulejów and Kłudzice) and have water quality monitoring posts (Sulejów and Przygłów). Below the dam is a water quality post, Smardzewice, and hydrological posts – Spała on the Pilica River and Zawada on the Wolbórka River (Figure 2). Hydrological gauges operated by the Institute of Meteorology and Water Management (IMGW) provide information on daily discharges. Water quality posts are operated by the Chief Inspectorate of Environmental Protection (GIOŚ) in a monthly sampling interval.
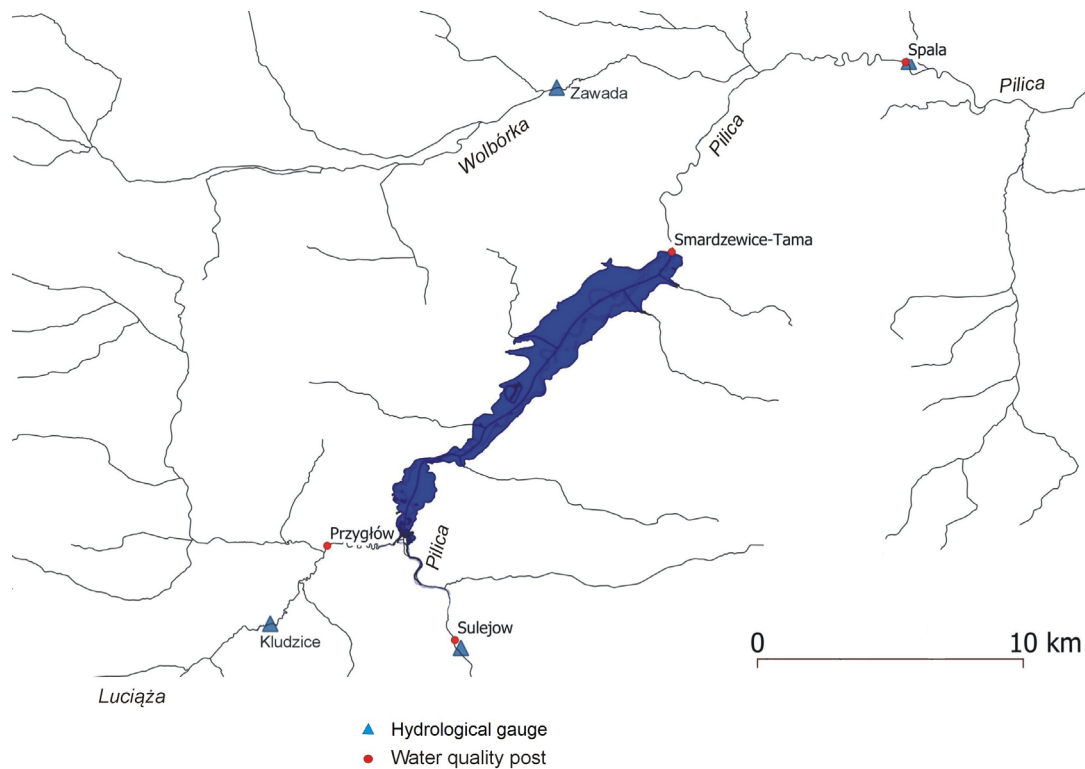

Figure 2. Location of the IMGW hydrological gauges and water GIOŚ quality monitoring stations of Sulejów Reservoir.

Long-term observations of Total Phosphorus (TP) concentrations may characterize the state of the Pilica River. Figure 3 shows average annual concentrations of TP at three monitoring points for the 1992–2010 period – Sulejów and Przygłów at the reservoir inlet, and Smardzewice below the dam. The improvement in water quality is visible, especially after 2004, which corresponds with Poland's accession to the European Union and the adoption of Water Directive recommendations, combined with extensive investment in developing municipal sewage treatment plants. The decrease in TP concentrations from the Luciąża River, controlled by the Przygłów monitoring station, is noticeable.

The Sulejów Reservoir plays an essential role in the self-purification of the Pilica River, improving the water quality in the river downstream but creating the problem of eutrophication in the reservoir. Long-term water retention in the reservoir is favourable for sedimentation, and reduction of both Total Phosphorus TP and Total Nitrogen (TN)   [25].

A study by [26] has shown that the Sulejów reservoir was a trap for suspended particulate matter (SPM). In 2006, the mean inflow concentration of SPM in the backwater area was 13.56 mg dm^{-3} and the mean outflow concentration was 7.48 mg dm^{-3}. The research showed an annual significant reduction of nutrients and SPM concentrations and retention in the reservoir compared with 1992, which amounted to 28% of TP, 34% of TN, and 45% of SPM.
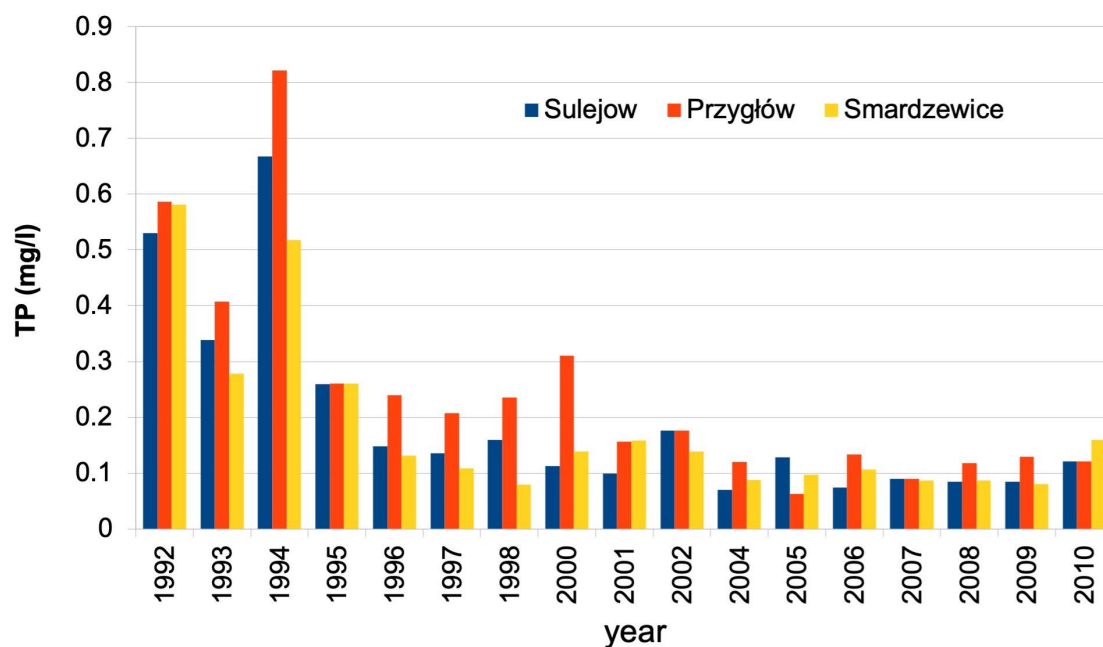

Figure 3. Average annual concentrations of TP in the monitoring stations at the Sulejów Reservoir backwater (Pilica River – Sulejów, Luciąża River – Przygłów) and below the Pilica dam – Smardzewice.

The period 2004–2009 is representative of the long-term water quality status of the Pilica and Luciąża rivers. Extreme flooding happened in 2010 when the discharge on the Pilica River at Sulejów gauge reached 223 m3s-1. TP loads are calculated at monthly intervals at the inlet to the reservoir and the outlet. The load is calculated by multiplying a product of TP concentration, measured at the GIOŚ water quality monitoring point, with average monthly discharge, measured at the IMGW hydrological gauges. At the inflow to the reservoir, discharge is measured at Sulejów and Kłudzice gauges, while TP concentration is measured at Sulejów and Przygłów monitoring points. The TP load at the outlet of the reservoir is calculated from concentrations measured at the Smardzewice monitoring point below the dam and the average monthly discharge from the Spała gauge minus the discharge from the Wolbórka River tributary, controlled at the Zawada gauge.

Monthly values of TP load at the inlet to the reservoir (Sulejów and Przygłów monitoring points) and at the outlet of the reservoir (Smardzewice monitoring point) together with average monthly

discharge values of Pilica and Luciąża rivers are shown at Figure 4. Additionally, the average discharge of Pilica and Luciąża rivers in July–September is marked.
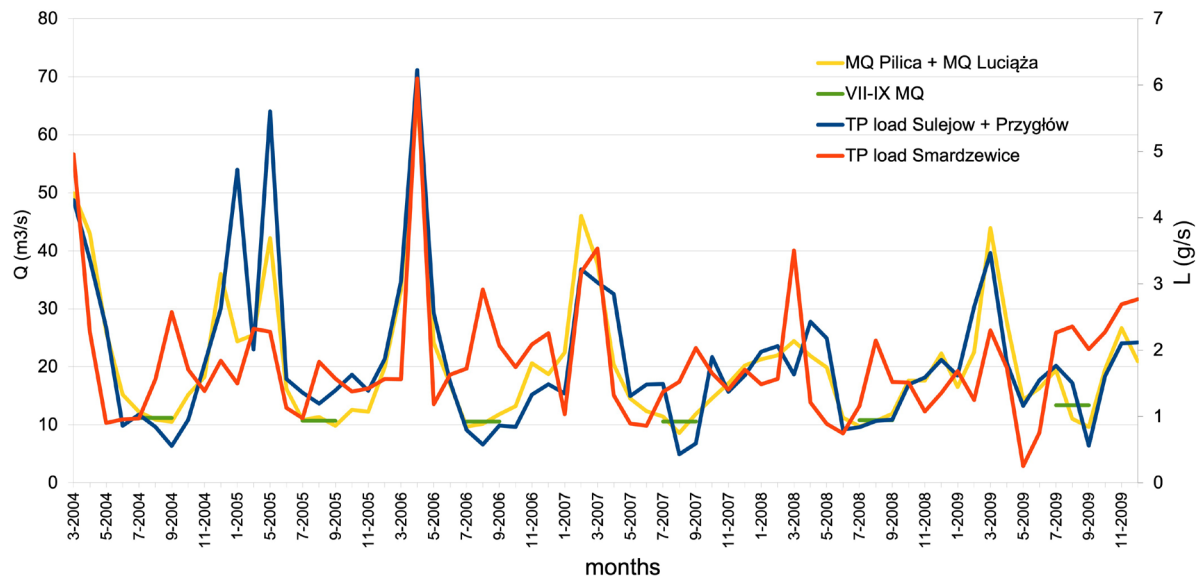

Figure 4. Monthly values of TP load at the inlet to the reservoir (Sulejów and Przygłów monitoring points) and at the outlet of the reservoir (Smardzewice) together with monthly discharge and average discharge in months July–September of Pilica and Luciąża rivers (VII-IX MQ).

An important process in phytoplankton bloom is the so-called internal loading, in which bottom sediments act as a source of nutrients. [27] measured chemicals from Sulejów Reservoir bottom sediments, including total organic carbon (TOC) and TP concentrations. They found that the highest amounts of biogenic components are deposited in sediments of the lacustrine zone and in sites where fine-size fractions prevail in the deposited material. In a study by [28], Sulejów Reservoir sedimentation areas with higher TP concentrations were found to be in the lacustrine zone, with the highest depths corresponding to the former Pilica River channel. High TP concentrations were also found in sediment traps in sheltered bays on the western coast of the lacustrine zone.

2.2. Remote sensing data

The distribution of phytoplankton bloom on the Sulejów Reservoir was documented using Sentinel-2 satellite images and the Normalized Difference Chlorophyll Index (NDCl). Using SNAP software, provided by ESA, a subset of samples representing the Sulejów Reservoir was extracted from the scenes. The remote sensing index NDCl was calculated using the formula described by [12]:

$$(B5-B4)/(B5+B4)$$

, where B5 and B4 are the band numbers of Sentinel-2 images.

The highest number of images on the Sulejow reservoir area available for the vegetation period, in cloud-free conditions, was in 2020 (Figure 5). As additional information, the wind conditions (direction and force) at the moment of image sensing were obtained from IMGW meteorological stations.
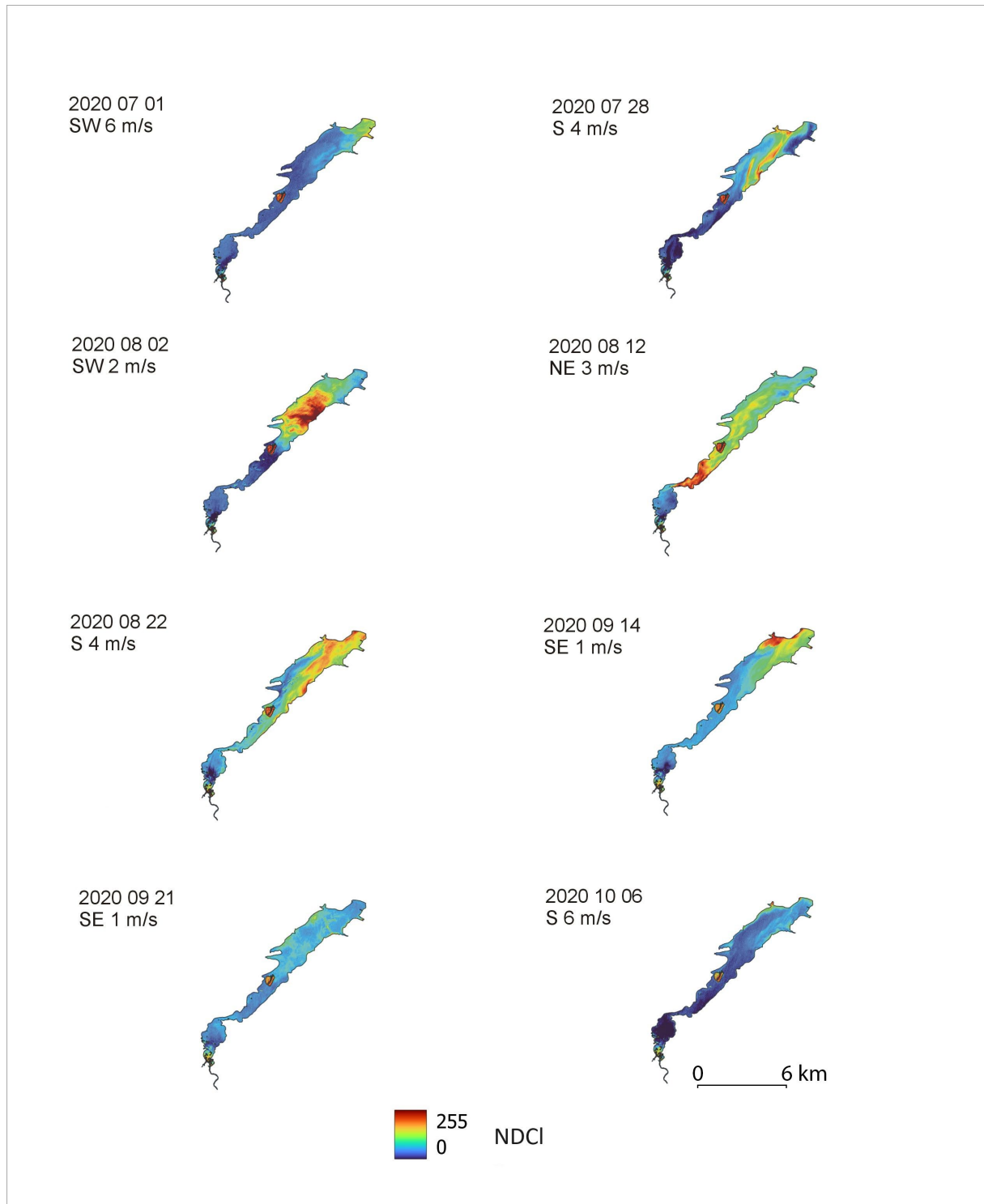
Figure 5. Distribution of phytoplankton bloom on the Sulejów Reservoir: documented using NDCl index, calculated from bands B4 and B5 of Sentinel-2 satellite images. Below the date of image recording, simultaneous wind direction and force are given.

Calculated for every eight images, remote sensing indexes NDCl were arithmetically added, creating a map with accumulated values of the index. This map shows the most frequent and intensive occurrence of phytoplankton bloom at Sulejów Reservoir in 2020 (Figure 6).
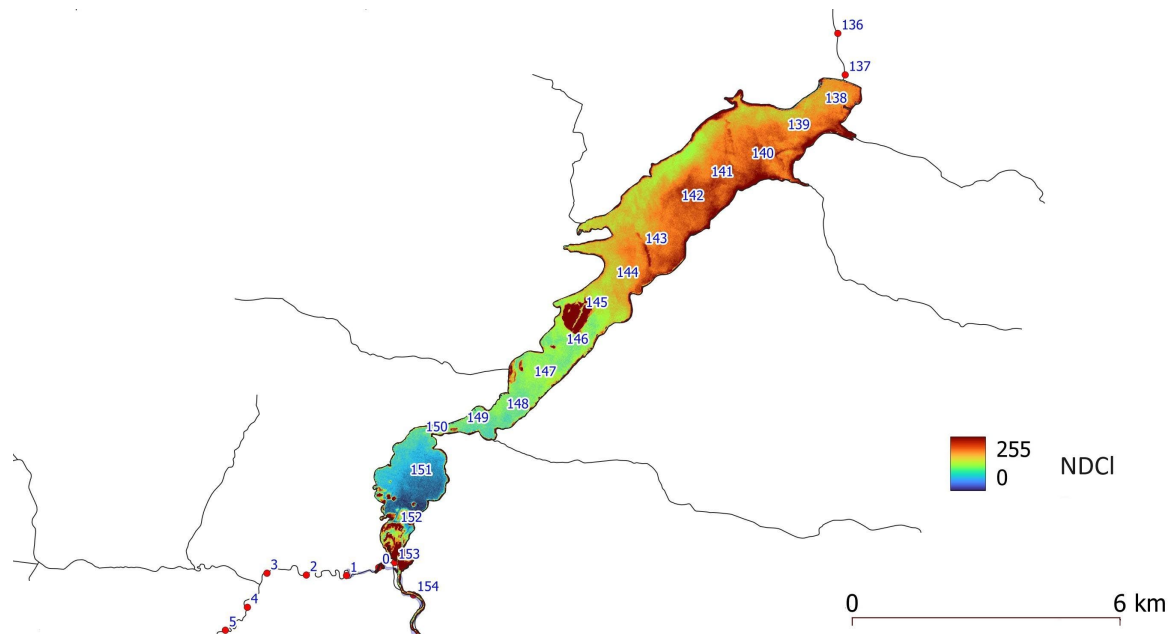
Figure 6. The sum of NDCl indexes, calculated from eight Sentinel-2 images recorded in the period 2020/07/01-2020/10/06, showing the most frequent and intensive occurrence of phytoplankton bloom on Sulejów Reservoir.

2.3. Hydrodynamic modelling

Wind action can also create secondary circulation patterns in the form of large eddies. To take this process into account, we used the CCHE2D hydrodynamic model developed at the National Center for Computational Hydroscience and Engineering (NCCHE) at the University of Mississippi, U.S.A., employing the finite elements method. This is a two-dimensional depth-averaged, unsteady, turbulent open-channel flow model based on the depth-averaged Navier-Stokes equations, incorporating the impact of wind on water surfaces, so the model may be used for cases in which water flow is affected by the wind field. Examples of CCHE2D use for rivers and reservoirs may be found in previous works [20,21,29–31]. A detailed description of the model may be found in [32].

The two-dimensional computational grid and bed profile necessary to perform the velocity simulations were prepared using the CCHE_MESH generator developed by NCCHE. The final computing mesh had a dimension of I=80 x J=700 elements. The simulations were run for 60-second time steps. The geometry of the reservoir was calculated from a 5 m resolution DTM (Digital Terrain Model), based on a precise bathymetric plan measured by [33]. The upper boundary condition was the discharge of the Pilica River and Luciąża River, and the lower boundary condition was a water head at the dam profile. All boundary conditions for the simulation of water flow and wind action were obtained from the IMGW hydrological and meteorological stations.

3. Results and Discussion

The distribution of phytoplankton bloom shows that its cover, using the NDCl index, starts to develop in July near the dam in the lacustrine zone, develops to maximum levels in August, and then slowly diminishes at the beginning of October (Figure 5).

Long-term analysis of the water quality of the Pilica and Luciąża rivers shows slow improvement, expressed in a decrease in TP concentrations in both rivers in the post-2004 period (Figure 3). Despite the trend in the water quality of the Pilica and Luciąża rivers, Sentinel-2 images register intensive phytoplankton bloom on the Sulejów Reservoir every year. Our study focuses on the year 2020, for which we obtained eight cloud-free images, allowing us to use the NDCl remote sensing index to visualize phytoplankton intensity and distribution on the reservoir.

Attempts were made to find the relation between NDCl index values and chlorophyll-a concentrations. The problem encountered in a lot of research is that spectral channels in the blue-green part of the electromagnetic spectrum are heavily affected by the presence of constituents such as Colored Dissolved Organic Matter (CDOM), detritus, tripton, and suspended sediment [12]. In this study, we use the NDCl index to determine the spatial range and intensity of phytoplankton bloom. The sum of the values of the NDCl indexes, calculated from the eight images, shows where the phytoplankton occurs most frequently. The most intensive occurrence of phytoplankton bloom is found in a lacustrine zone of the Sulejów Reservoir between kilometres 137 and 145.

The distribution of phytoplankton bloom cover shows that it starts to develop in July near the dam and reaches maximum levels in August, then starts to diminish at the beginning of October. The long water-retention time, low-flow stagnant water with low velocity in the lacustrine zone, and high water temperature promote the intensive bloom of phytoplankton during that period.

The comparison of TP loads at the inflow and outflow of the reservoir shows that, during the summer months and low-flow conditions, the reservoir acts as a source of nutrients. The TP load leaving the reservoir through the dam spill is higher than the inflow from the Pilica and Luciąża rivers (Figure 4). This can be explained by the fact that phytoplankton biomass contains an organic part of TP, which is transported by the flow of water through the reservoir.

The sum of the NDCl index, calculated from eight Sentinel-2 images (period July–October 2020), shows that the place of most intensive and frequent phytoplankton bloom is the lacustrine part of the Sulejów Reservoir. This pattern corresponds with bottom sediment samples having the highest concentration of TP, located in the area of the former Pilica River Thalweg at the lacustrine zone [27,28] (Figure 7). That part of the reservoir's bottom sediments has a large pool of TP and may act as an internal loading mechanism, supplying cyanobacteria with phosphorus during the phytoplankton bloom.
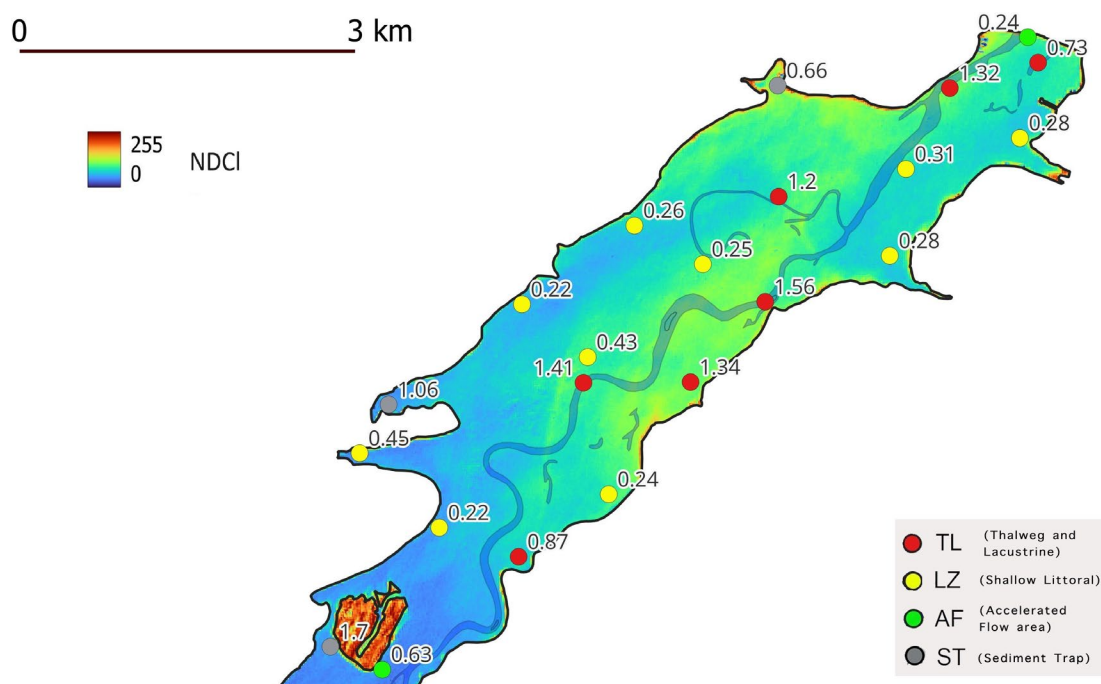

Figure 7. Sulejów Reservoir lacustrine zone; summarized NDCl index, calculated from eight Sentinel-2 images, and concentration of TP in bottom sediments with different sedimentation conditions.

In the lacustrine part of the reservoir, the flow velocities are very low, and the water circulation pattern is controlled not only by reservoir geometry but also by wind. Two cases were studied representing the influence of wind direction SW and NE and calculated using the CCHE2D model.

The influence of wind – SW direction (blowing downstream) and force 2 m s-1 – on the distribution of phytoplankton, expressed by the NDCl index on 2020/08/02, is shown in Figure 8. Similarly, the NDCl index, calculated for the Sentinel-2 image from 2020/08/12 and the velocity field created by wind blowing upstream from NE direction and force 3 m s-1, is shown in (Figure 9).
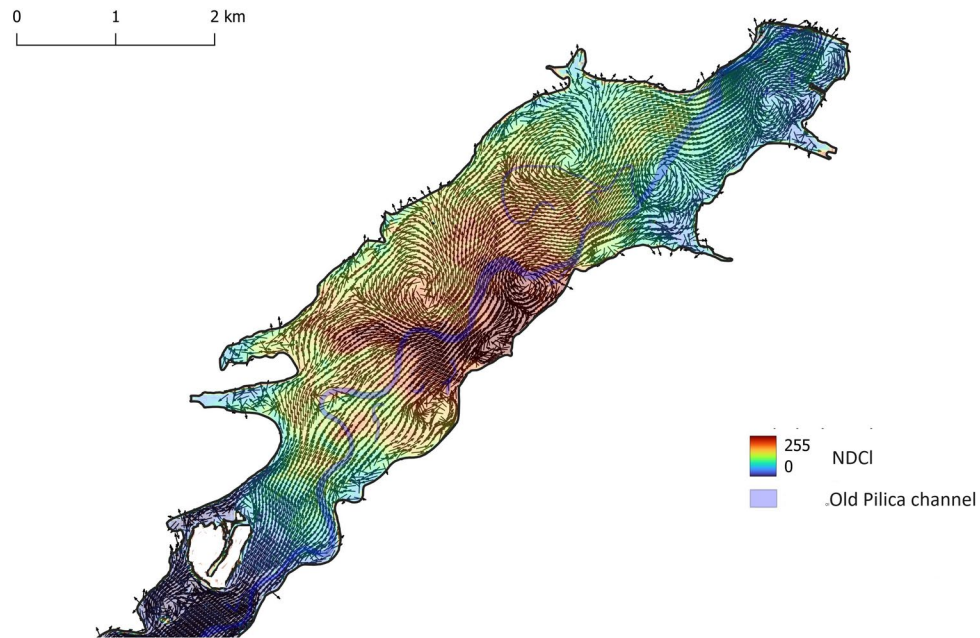

Figure 8. Lacustrine part of Sulejów Reservoir – NDCl index, calculated from Sentinel-2 image from 2020/08/02, and velocity field of surface currents, calculated using CCHE2D model at wind direction SW and force 2 m s-1.
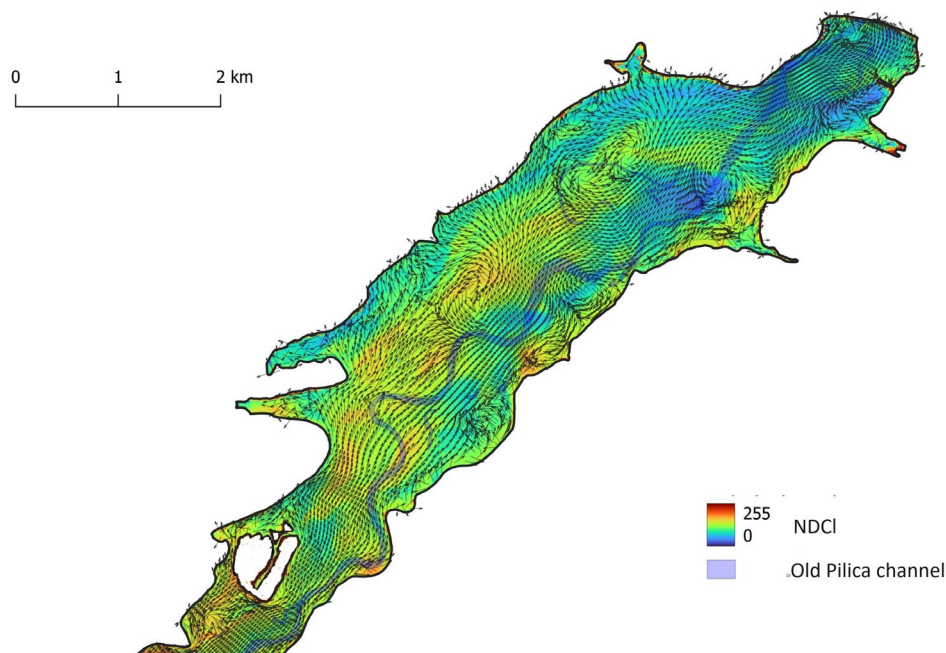
Figure 9. Lacustrine part of Sulejów Reservoir – NDCl index, calculated for Sentinel-2 image from 2020/08/12, and velocity field of surface currents, calculated using CCHE2D model at wind direction NE and force 3 m s^{-1}.

Both cases show that large vortices, creating circulation patterns at places of convergence, create higher concentrations of phytoplankton. Vortices forming at the right bank of the reservoir near-shore expansion near the dam are located away from the former Pilica River thalweg and do not create convergence zones,   that would increase the concentration of the phytoplankton.

The lower values of NDCl in the lacustrine zone of the Sulejów Reservoir, in the image from 2020/08/12, are caused by an NE wind that pushed phytoplankton upstream to transitional and riverine zones (see Figure 6).

A similar approach in larger-scale oceanographic studies was used by [34] who selected seven years (1998–2004) of remotely sensed data to create monthly climatological fields, and numerically simulated the spatiotemporal characteristics of chlorophyll-a in the waters of Porcupine and Rockall Bank in the north-eastern Atlantic.

[35] combined hydrodynamic modelling with remote sensing data to develop a hydrodynamic model of algal bloom transport for Lake Erie, and remotely sensed chlorophyll-a data from the European Space Agency's Sentinel-3A OLCI sensor.

Some studies tried to monitor SPM by comparing satellite remote sensing retrieval with numerical simulation. [36] modelled SPM distribution using a coupled hydrodynamic and dispersion model and analysis of Landsat TM data in Laguna de Terminos, Campeche, Mexico.

[37] combined MERIS satellite remote sensing data with numerical modelling to study Pakri Bay in the southern Gulf of Finland to improve the understanding of sediment dynamics. The results show good agreement with the in-situ measurements and simulated SPM dynamics in clear waters, with an SPM concentration of lower than 20 mg dm^{-3}.

Remote sensing data on chlorophyll-a and suspended sediment distribution can also be used to verify hydrodynamic models. The pattern of sediment flux from the river to the reservoir is visible

on multispectral and hyperspectral images and may be compared to the field of suspended sediment concentration calculated by the 2D model [38].

4. Conclusions

In the case of the eutrophication of reservoirs built on rivers, the important question is to what extent high concentrations of phytoplankton in the reservoir's lacustrine zone depend on the TP flux. The hydraulic properties of the Sulejów Reservoir create favourable conditions for sedimentation and storage of TP [26], so the reservoir, in a long time horizon, acts as a sink for SPM and nutrients. Calculation of TP load has shown that, in conditions of low flow during the summer months, the reservoir can act as a source in July–September, supplying the lower reach of the Pilica River with TP due to the high concentration of the organic form of phosphorus enclosed in a phytoplankton bloom in the lacustrine part of the reservoir.

Sulejów Reservoir is a large water body and, because of that, standard water quality measurements are performed in monitoring stations located along the reservoir's longitudinal profile. Remote sensing using multispectral satellite images opens new opportunities in hydrobiological and ecological studies. The drawback for detecting the intensity and location of phytoplankton bloom on reservoirs in middle latitude regions is cloud cover, which makes the optical satellite images unsuitable.

Coupling remote sensing data and numerical modelling helps verify the hydrodynamic model results and understand nutrients and sediment dynamics. Hydrodynamic modelling helps interpret the remote sensing data and can be useful for selecting suitable places for ground measurements at water quality monitoring stations.

The water quality monitoring system, which consists of ground stations, gives a limited picture of important water properties such as SPM and chlorophyll-a concentrations. The spatial pattern of these parameters can be understood with the help of remote sensing data and hydrodynamic modelling.

References

1. Harper, D.M. *Eutrophication of Freshwaters: Rinciples, Problems, and Restoration*; 1st ed.; Chapman & Hall: London ; New York, 1992; ISBN 978-0-412-32970-8.

2. Yoshimura, S. Rapid Entrophication within Recent Years of Lake Haruna, Gunma, Japan. *Jpn. J. Geol. Geogr.* **1933**, *11*, 31–41.

3. Kornijów, R. Eutrophication and Derivative Concepts. Origins, Compatibility and Unresolved Issues. *Ecohydrol. Hydrobiol.* **2023**, S1642359323000708, doi:10.1016/j.ecohyd.2023.07.001.

4. Schindler, D.W. The Dilemma of Controlling Cultural Eutrophication of Lakes. *Proc. R. Soc. B Biol. Sci.* **2012**, *279*, 4322–4333, doi:10.1098/rspb.2012.1032.

5. Szczukocki, D.; Krawczyk, B.; Dałkowski, R.; Juszczak, R.; Miekoś, E.; Zieliński, M.; Cieśliński, R.; Jereczek-Korzeniewska, K. *Monitoring hydrochemiczny zbioeników zaporowych województw łódzkiego*; Problemy badań wody w XX I XXI wieku.; Wydawnictwo Uniwersytetu Gdańskiego: Gdańsk, 2014;

6. Zanchett, G.; Oliveira-Filho, E. Cyanobacteria and Cyanotoxins: From Impacts on Aquatic Ecosystems and Human Health to Anticarcinogenic Effects. *Toxins* **2013**, *5*, 1896–1917, doi:10.3390/toxins5101896.

7. Tarczyńska, M.; Osiecka, R.; Kątek, R.; Błaszczyk, A.; Zalewski, M. *Przyczyny i konsekwencje powstawania toksycznych zakwitów sinicowych w zbiornikach*; Zastosowanie biotechnologii ekosystemalnych do poprawy jakości wód.; Instytut Ekologii PAN, Człowiek i środowisko, 1997; Vol. 18;.

8. Ryan, J.; Greenfield, D.; Marin, R., Iii; Preston, C.; Roman, B.; Jensen, S.; Pargett, D.; Birch, J.; Mikulski, C.; Doucette, G.; et al. Harmful Phytoplankton Ecology Studies Using an Autonomous Molecular Analytical and Ocean Observing Network. *Limnol. Oceanogr.* **2011**, *56*, 1255–1272, doi:10.4319/lo.2011.56.4.1255.

9. Hadjimitsis, D.G.; Clayton, C. Assessment of Temporal Variations of Water Quality in Inland Water Bodies Using Atmospheric Corrected Satellite Remotely Sensed Image Data. *Environ. Monit. Assess.* **2009**, *159*, 281–292, doi:10.1007/s10661-008-0629-3.

10. Palmer, S.C.J.; Kutser, T.; Hunter, P.D. Remote Sensing of Inland Waters: Challenges, Progress and Future Directions. *Remote Sens. Environ.* **2015**, *157*, 1–8, doi:10.1016/j.rse.2014.09.021.

11. Kutser, T.; Metsamaa, L.; Strömbeck, N.; Vahtmäe, E. Monitoring Cyanobacterial Blooms by Satellite Remote Sensing. *Estuar. Coast. Shelf Sci.* **2006**, *67*, 303–312, doi:10.1016/j.ecss.2005.11.024.

12. Mishra, S.; Mishra, D.R. Normalized Difference Chlorophyll Index: A Novel Model for Remote Estimation of Chlorophyll-a Concentration in Turbid Productive Waters. *Remote Sens. Environ.* **2012**, *117*, 394–406, doi:10.1016/j.rse.2011.10.016.

13. Glibert, P.M.; Anderson, D.A.; Gentien, P.; Graneli, E.; Sellner, K.G. The Global, Complex Phenomena of Harmful Algal Blooms. *Oceanogr. Soc.* **2005**, *182*.

14. Paerl, H.W. Nuisance Phytoplankton Blooms in Coastal, Estuarine, and Inland Waters1. *Limnol. Oceanogr.* **1988**, *33*, 823–843, doi:10.4319/lo.1988.33.4part2.0823.

15. Carrick, H.J.; Worth, D.; Marshall, M.L. The Influence of Water Circulation on Chlorophyll-Turbidity Relationships in Lake Okeechobee as Determined by Remote Sensing. *J. Plankton Res.* **1994**, *16*, 1117–1135, doi:10.1093/plankt/16.9.1117.

16. Kawara, O.; Yura, E.; Fujii, S.; Matsumoto, T. A Study on the Role of Hydraulic Retention Time in Eutrophication of the Asahi River Dam Reservoir. *Water Sci. Technol.* **1998**, *37*, doi:10.1016/S0273-1223(98)00030-4.

17. Tufford, D.L.; McKellar, H.N. Spatial and Temporal Hydrodynamic and Water Quality Modeling Analysis of a Large Reservoir on the South Carolina (USA) Coastal Plain. *Ecol. Model.* **1999**, *114*, 137–173, doi:10.1016/S0304-3800(98)00122-7.

18. Verkhozina, V.A.; Kozhova, O.M.; Kusner, Yu.S. Hydrodynamics as a Limiting Factor in the Lake Baikal Ecosystem. *Aquat. Ecosyst. Health Manag.* **2000**, *3*, 203–210, doi:10.1080/14634980008657015.

19. Hama Karim, P.; Ziemińska-Stolarska, A.; Magnuszewski, A. Hydraulic Properties of Sulejów Reservoir in Poland as a Driving Factor of Sedimentation Processes. In *GeoPlanet: Earth and Planetary Sciences*; Springer International Publishing, 2023; p. (in Press).

20. Magnuszewski, A.; Moran, S.; Yu, G. Modelling Lowland Reservoir Sedimentation Conditions and the Potential Environmental Consequences of Dam Removal: Wloclawek Reservoir, Vistula River, Poland. *IAHS Publ.* **2010**, 345–352.

21. Magnuszewski, A.; Sabat, A.; Jarocińska, A.; Sławik, Ł. Application of the AISA Hyperspectral Image for Verification of Sediment Transport Results Obtained from CCHE2D Hydrodynamic Model—Zegrze Reservoir Case Study, Poland. In *Free Surface Flows and Transport Processes*; Kalinowska, M.B., Mrokowska, M.M., Rowiński, P.M., Eds.; GeoPlanet: Earth and Planetary Sciences; Springer International Publishing: Cham, 2018; pp. 103–112 ISBN 978-3-319-70913-0.

22. Ziemińska-Stolarska, A.; Polańczyk, A.; Zbiciński, I. 3-D CFD Simulations of Hydrodynamics in the Sulejow Dam Reservoir. *J. Hydrol. Hydromech.* **2015**, *63*, 334–341, doi:10.1515/johh-2015-0033.

23. Magnuszewski, A.; Kiedrzyńska, E.; Kiedrzyński, M.; Moran, S. Gis Approach to Estimation of the Total Phosphorous Transfer in the Pilica River Lowland Catchment. *Quaest. Geogr.* **2014**, *33*, 101–110, doi:10.2478/quageo-2014-0033.

24. Pieron, Ł.; Absalon, D.; Habel, M.; Matysik, M. Inventory of Reservoirs of Key Significance for Water Management in Poland—Evaluation of Changes in Their Capacity. *Energies* **2021**, *14*, 7951, doi:10.3390/en14237951.

25. Kiedrzyńska, E.; Kiedrzyński, M.; Urbaniak, M.; Magnuszewski, A.; Skłodowski, M.; Wyrwicka, A.; Zalewski, M. Point Sources of Nutrient Pollution in the Lowland River Catchment in the Context of the Baltic Sea Eutrophication. *Ecol. Eng.* **2014**, *70*, 337–348, doi:10.1016/j.ecoleng.2014.06.010.

26. Urbaniak, M.; Kiedrzyńska, E.; Zalewski, M. The Role of a Lowland Reservoir in the Transport of Micropollutants, Nutrients and the Suspended Particulate Matter along the River Continuum. *Hydrol. Res.* **2012**, *43*, 400–411, doi:10.2166/nh.2012.108.

27. Ziemińska-Stolarska, A.; Imbierowicz, E.; Jaskulski, M.; Szmidt, A. Assessment of the Chemical State of Bottom Sediments in the Eutrophied Dam Reservoir in Poland. *Int. J. Environ. Res. Public. Health* **2020**, *17*, 3424, doi:10.3390/ijerph17103424.

28. Hama Karim, P.; Ziemińska-Stolarska, A.; Magnuszewski, A. Hydraulic Control on Sedimentation Processes and Bottom Sediments Chemistry of Sulejów Reservoir in Poland. *Misc. Geogr.* **2024**, *10.2478/mgrsd-2023–0029*, (in press).

29. Kalinowska, M.B.; Rowiński, P.M.; Kubrak, J.; Mirosław-Świątek, D. Scenarios of the Spread of a Waste Heat Discharge in a River — Vistula River Case Study. *Acta Geophys.* **2012**, *60*, 214–231, doi:10.2478/s11600-011-0045-x.

30. Kalinowska, M.B.; Rowiński, P.M. Uncertainty in Computations of the Spread of Warm Water in a River – Lessons from Environmental Impact Assessment Case Study. *Hydrol. Earth Syst. Sci.* **2012**, *16*, 4177–4190, doi:10.5194/hess-16-4177-2012.

31. Altinakar, M.; Czernuszenko, W.; Rowiński, P.; Wang, S. *Computational Modeling for the Development of Sustainable Water-Resources Systems in Poland. US-Poland Technology Transfer Program*; E; Institute of Geophysics, Polish Academy of Sciences: Warsaw, 2005; Vol. E-5 (387);

32. Jia, Y; Wang, S. CCHE2D: Two-Dimensional Hydrodynamic and Sediment Transport Model for Unsteady Open Channel Flows over Loose Bed, Technical Report No. NCCHE-TR-2001-1 2001.

33. Jaskulski, M.; Szmidt A.; Zbiciński I.; Ziemińska-Stolarska A.; Adamiec J. Konstrukcja mapy batymetrycznej na podstawie badań sonarowych sztucznego zbiornika wodnego na przykładzie Zalewu Sulejowskiego. *Teledetekcja Śr.* **2018**, *59*, 5–12.

34. Mohn, C.; White, M. Remote Sensing and Modelling of Bio-Physical Distribution Patterns at Porcupine and Rockall Bank, Northeast Atlantic. *Cont. Shelf Res.* **2007**, *27*, 1875–1892, doi:10.1016/j.csr.2007.03.006.

35. Soontiens, N.; Binding, C.; Fortin, V.; Mackay, M.; Rao, Y.R. Algal Bloom Transport in Lake Erie Using Remote Sensing and Hydrodynamic Modelling: Sensitivity to Buoyancy Velocity and Initial Vertical Distribution. *J. Gt. Lakes Res.* **2019**, *45*, 556–572, doi:10.1016/j.jglr.2018.10.003.

36. Jensen, J.R.; Kjerfve, B.; Ramsey, E.W.; Magill, K.E.; Medeiros, C.; Sneed, J.E. Remote Sensing and Numerical Modeling of Suspended Sediment in Laguna de Terminos, Campeche, Mexico. *Remote Sens. Environ.* **1989**, *28*, 33–44, doi:10.1016/0034-4257(89)90103-X.

37. Kouts, T.; Sipelgas, L.; Savinits, N.; Raudsepp, U. Environmental Monitoring of Water Quality in Coastal Sea Area Using Remote Sensing and Modeling. In Proceedings of the 2006 IEEE US/EU Baltic International Symposium; IEEE: Klaipeda, Lithuania, May 2006; pp. 1–8.

38. Sabat-Tomala, A.; Jarocińska, A.M.; Zagajewski, B.; Magnuszewski, A.S.; Sławik, Ł.M.; Ochtyra, A.; Raczko, E.; Lechnio, J.R. Application of HySpex Hyperspectral Images for Verification of a Two-Dimensional Hydrodynamic Model. *Eur. J. Remote Sens.* **2018**, *51*, 637–649, doi:10.1080/22797254.2018.1470905.